

# Landau Gauge Gluon and Ghost Propagators from Lattice QCD \*

E.-M. Ilgenfritz, M. Müller-Preussker, A. Sternbeck<sup>†</sup>

*Humboldt-Universität zu Berlin, Institut für Physik, Newtonstr. 15, 12489 Berlin, Germany*

A. Schiller

*Universität Leipzig, Institut für Theoretische Physik, Vor dem Hospitaltore 1, 04103 Leipzig, Germany*

I. L. Bogolubsky

*Joint Institute for Nuclear Research, Dubna 141980, Russia*

(Received on October 24, 2006)

We report on recent numerical computations of the Landau gauge gluon and ghost propagators as well as of the ghost-gluon-vertex function in pure  $SU(3)$  Yang-Mills theory and in full QCD on the lattice. Special emphasis is paid to the low momentum region. In particular, we present new data for the gluon propagator at momenta below 300 MeV. We also discuss different systematic effects as there are finite-size, lattice discretization and Gribov copy but also unquenching effects. A MOM-scheme running coupling  $\alpha_s(q^2)$  based on the ghost-gluon vertex is calculated and found to decrease for momenta below 550 MeV, even though the renormalization constant of the vertex deviates only weakly from being constant.

PACS numbers: 11.15.Ha, 12.38.Gc, 12.38.Aw

Keywords: lattice gauge theory, Landau gauge, gluon propagator, ghost propagator, running coupling

## I. INTRODUCTION

With our contribution to this workshop we give an overview on recent lattice computations of the Landau gauge gluon and ghost propagators in quenched ( $N_f = 0$ ) and in full QCD ( $N_f = 2$ ). The full analysis and additional results of related observables can be found in the Ph.D. thesis of one of us [1].

For QCD being *the* theory of the strong interaction a coherent description of all hadronic features directly based on the dynamics of confined quarks and gluons, given in terms of all propagators and vertex functions of QCD, should be available. As reported by R. Alkofer at this conference, they may serve as an input from first principles for the Bethe-Salpeter and Faddeev equations and this opens a way to a model independent phenomenology of nonperturbative phenomena.

Lattice computations of gauge-variant Green functions have attracted more and more interest in recent years, because the results can be directly confronted with studies of continuous Dyson-Schwinger equations (DSE). Both nonperturbative approaches have their own limitations. Whereas the lattice approach is affected by finite-size and discretization errors, the DSE approach requires truncations of an infinite tower of equations and those truncations are difficult to control. Therefore, a comparison of results is eventually able to provide more confidence about the consistence of both approaches.

Starting with the work by L. von Smekal *et al.* [2, 3], DSE studies in recent years [4, 5, 6, 7, 8, 9, 10] have shown evidence for an intertwined infrared power behavior of the gluon

and ghost dressing functions

$$\begin{aligned} Z(q^2) &\equiv q^2 D(q^2) \propto (q^2)^{2\lambda}, \\ J(q^2) &\equiv q^2 G(q^2) \propto (q^2)^{-\lambda}, \end{aligned} \quad (1)$$

respectively, with the same value  $\lambda \approx 0.59$  [11, 12]. Thus, the gluon propagator  $D(q^2)$  would be vanishing in the infrared in close connection with a diverging ghost propagator  $G(q^2)$ . This infrared behavior is closely related to gluon and quark confinement in accordance with the Gribov-Zwanziger horizon condition [13, 14] and the Kugo-Ojima criterion [15].

As a by-product, a nonperturbative determination of the running coupling  $\alpha_s(q^2)$  in a momentum subtraction (MOM) scheme can be obtained. In fact, under the condition that the ghost-gluon-vertex renormalization function  $Z_1(\mu^2)$  is finite and constant (see [16, 17] and [18] for a recent  $SU(2)$  lattice study) the corresponding running coupling is defined by

$$\alpha_s(q^2) = \frac{g^2}{4\pi} Z(q^2) J^2(q^2). \quad (2)$$

This together with relation (1) provides a non-trivial fixed point of  $\alpha_s$  in the infrared limit [11], which was also proposed by D. V. Shirkov on the basis of a perturbative analytic approach (see [19] and references therein).

For quenched  $SU(2)$  extensive lattice investigations of the gluon and ghost propagators in Landau gauge can be found in [20]. For  $SU(3)$  lattice computations of the gluon propagators were reported already in [21, 22, 23, 24]. Later, other groups focused on the ghost propagator [25, 26, 27], too. In our study we first paid special attention to the Gribov copy problem [28]. In the latter context we have also investigated spectral properties of the Faddeev-Popov operator [29]. With increasing physical volume we have found the low-lying eigenmode spectrum becoming steeper at the lowest non-zero eigenvalues. This hopefully closes the gap from the trivial zero eigenvalues and leads to a non-vanishing spectral density at zero

\*Talk presented at the Workshop IRQCD '06, Rio de Janeiro, May 2006 by M. Müller-Preussker.

<sup>†</sup>Address since Sept. 1, 2006: CSSM, School of Chemistry & Physics, University of Adelaide, SA 5005, Australia.

in the thermodynamic limit which is required for an infrared diverging ghost propagator. Moreover, in [30] we have reported on a first  $SU(3)$  lattice computation of the ghost-gluon vertex at zero gluon momentum that lends confirmation (see below) for an almost constant ghost-gluon-vertex renormalization constant. This was shown earlier in [18] for the case of  $SU(2)$ .

Also investigations for the gluon and ghost propagator in full QCD have been reported [31, 32, 33]. We have extended our investigations to this case, too, using configurations generated with  $N_f = 2$  dynamical clover-improved Wilson fermions [34]. The lattice field configurations have been provided to us by the QCDSF collaboration [35, 36].

Finally, we only mention the analysis of some interrelated confinement criteria: a check of reflection positivity violation by the gluon propagator [37] and the computation of the Kugo-Ojima confinement parameter [38]. Our own checks of these issues (see [1]) have led to similar observations and will be published elsewhere [39].

## II. LANDAU GAUGE, LATTICE GLUON AND GHOST PROPAGATORS

The  $SU(3)$  lattice gauge field configurations  $U = \{U_{x,\mu}\}$  have been generated by a standard (Hybrid) Monte Carlo algorithm and then put into the Landau gauge by iteratively maximizing the gauge functional

$$F_U[g] = \frac{1}{4V} \sum_x \sum_{\mu=1}^4 \text{Re Tr } {}^g U_{x,\mu}, \quad {}^g U_{x,\mu} = g_x U_{x,\mu} g_{x+\hat{\mu}}^\dagger \quad (3)$$

with  $g_x \in SU(3)$ . In general there are numerous local maxima (Gribov copies), each satisfying the lattice Landau gauge condition

$$(\partial_\mu {}^g A_\mu)(x) \equiv \sum_\mu ({}^g A_\mu(x + \hat{\mu}/2) - {}^g A_\mu(x - \hat{\mu}/2)) = 0 \quad (4)$$

for the gauge transformed lattice potential

$${}^g A_\mu(x + \hat{\mu}/2) = \frac{1}{2i} \left( {}^g U_{x,\mu} - {}^g U_{x,\mu}^\dagger \right) \Big|_{\text{traceless}}. \quad (5)$$

To explore to what extent this ambiguity has a significant influence on gauge dependent observables, for lattice sizes up to  $24^4$  we have gauge fixed each thermalized configuration a certain number of times (several tens depending on the lattice size and coupling constant) employing the *over-relaxation* algorithm and starting always from purely random gauge copies. Then for each configuration  $U$ , we have selected the first (fc) and the best (bc) gauge copy (best with respect to the functional value) for subsequent measurements. For details we refer to [28]. On lattices sizes larger than  $24^4$  we have restricted ourselves only to *one* copy per thermalized configuration (only fc copies). On those lattices we have applied also the *Fourier accelerated* method for fixing  $U$  to the Landau gauge.

The momentum space gluon propagator  $D_{\mu\nu}^{ab}(q^2)$  is the correlator of two Fourier transforms  $\tilde{A}_\mu^a(k)$  of the lattice potential  ${}^g A_\mu(x + \hat{\mu}/2)$  (the symbol  ${}^g$  is dropped from now on)

$$\begin{aligned} D_{\mu\nu}^{ab}(q^2) &= \left\langle \tilde{A}_\mu^a(k) \tilde{A}_\nu^b(-k) \right\rangle \\ &= \delta^{ab} \left( \delta_{\mu\nu} - \frac{q_\mu q_\nu}{q^2} \right) D(q^2), \end{aligned} \quad (6)$$

where  $q$  denotes the ‘‘physical’’ momentum

$$q_\mu(k_\mu) = \frac{2}{a} \sin \left( \frac{\pi k_\mu}{L_\mu} \right) \quad (7)$$

related to the integer valued lattice momentum  $k_\mu \in (-L_\mu/2, L_\mu/2]$  for the linear lattice extensions  $L_\mu, \mu = 1, \dots, 4$ . According to Ref. [22], a subset of admissible lattice momenta  $k$  has been chosen for the final analysis of the gluon (and ghost) propagator, although the Fast Fourier Transform algorithm easily provides us with all lattice momenta.

The ghost propagator is derived from the Faddeev-Popov (F-P) operator, the Hessian with respect to  $g_x$  of the gauge functional given in Eq. (3). It can be written in terms of the (gauge fixed) link variables  $U_{x,\mu}$  as

$$M_{xy}^{ab} = \sum_\mu A_{x,\mu}^{ab} \delta_{x,y} - B_{x,\mu}^{ab} \delta_{x+\hat{\mu},y} - C_{x,\mu}^{ab} \delta_{x-\hat{\mu},y} \quad (8)$$

$$\text{with } A_{x,\mu}^{ab} = \text{Re Tr} \left[ \{T^a, T^b\} (U_{x,\mu} + U_{x-\hat{\mu},\mu}) \right],$$

$$B_{x,\mu}^{ab} = 2 \cdot \text{Re Tr} \left[ T^b T^a U_{x,\mu} \right],$$

$$C_{x,\mu}^{ab} = 2 \cdot \text{Re Tr} \left[ T^a T^b U_{x-\hat{\mu},\mu} \right]$$

and  $T^a, a = 1, \dots, 8$  being the (hermitian) generators of the  $su(3)$  Lie algebra satisfying  $\text{Tr} [T^a T^b] = \delta^{ab}/2$ . The ghost propagator is then determined by inverting the F-P operator  $M$

$$G^{ab}(q) = \frac{1}{V} \sum_{x,y} \left\langle e^{-2\pi i k \cdot (x-y)} [M^{-1}]_{xy}^{ab} \right\rangle_U = \delta^{ab} G(q^2). \quad (9)$$

Following Refs. [40, 41] we have used the conjugate gradient (CG) algorithm to invert  $M$  on a plane wave  $\tilde{\Psi}_c$  with color and position components  $\Psi_c^a(x) = \delta^{ac} \exp(2\pi i k \cdot x)$ . In fact, we applied a pre-conditioned CG algorithm (PCG) to solve  $M_{xy}^{ab} \phi^b(y) = \Psi_c^a(x)$ . As the pre-conditioning matrix we used the inverse Laplacian operator  $\Delta^{-1}$  with a diagonal color substructure. This has significantly reduced the required amount of computing time (for details see [28]).

## III. PROPAGATORS: QUENCHED AND FULL QCD RESULTS

For the pure  $SU(3)$  Yang-Mills case we have generated the gauge fields using the standard Wilson plaquette action for bare coupling values  $\beta = 6/g_0^2 = \{5.7, 5.8, 6.0, 6.2\}$ . Studying very large lattices (up to lattice size  $56^4$ ) at the smallest

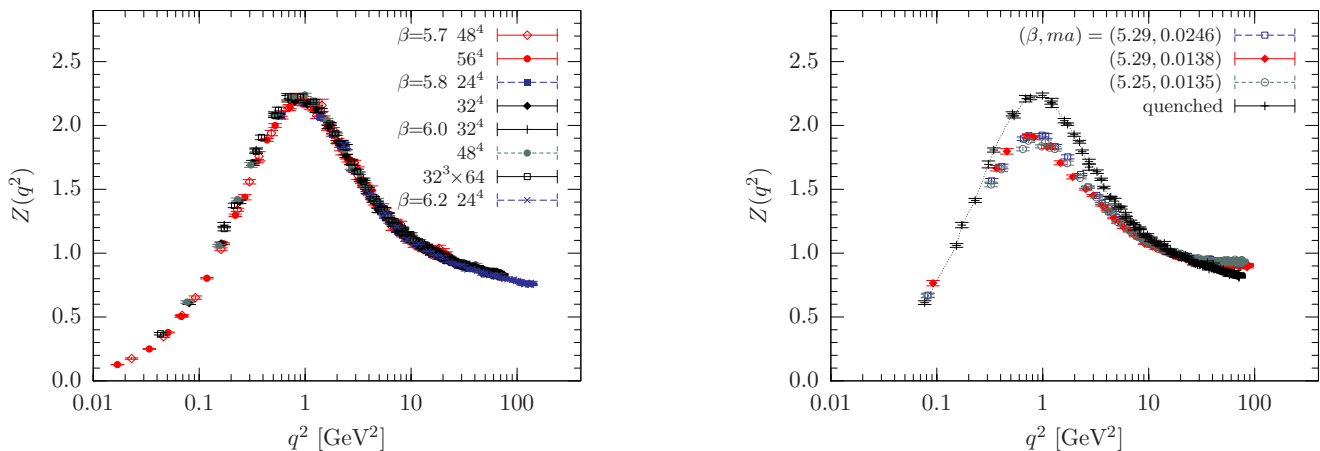


FIG. 1: The dressing functions for the gluon propagator  $Z(q^2) \equiv q^2 D(q^2)$  vs.  $q^2$  for quenched QCD (l.h.s.) and full QCD (r.h.s.), both measured on  $f_c$  gauge copies. To illustrate the unquenching effect some quenched QCD data ( $\beta = 6.0$ ,  $32^4$  and  $48^4$ ) are shown in the right figure, too.

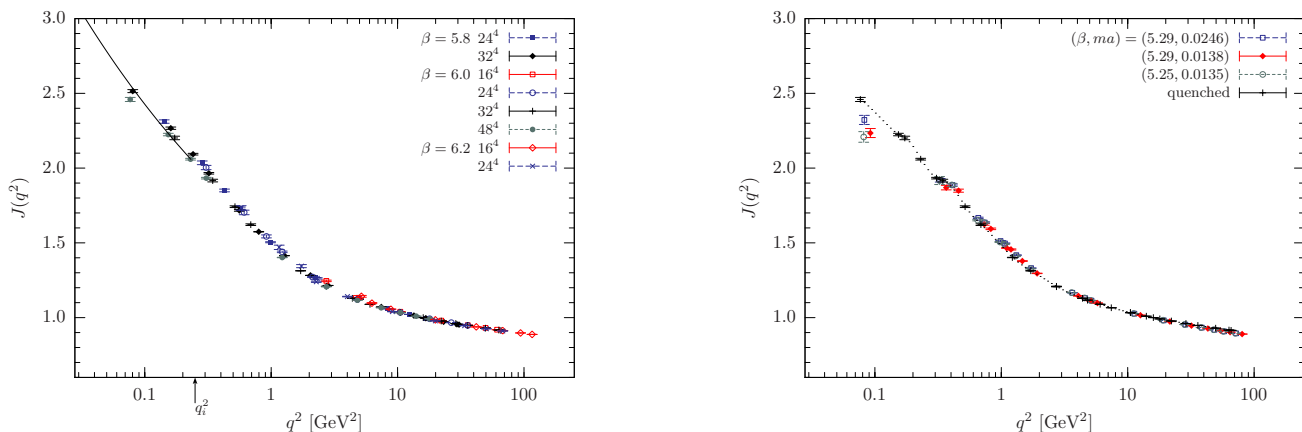


FIG. 2: As Fig. 1, here for the dressing function of the ghost propagator  $J(q^2) \equiv q^2 G(q^2)$ . The line (l.h.s.) represents a fit to the data for momenta lower than  $q_i^2$  using the power law given in relation (1).

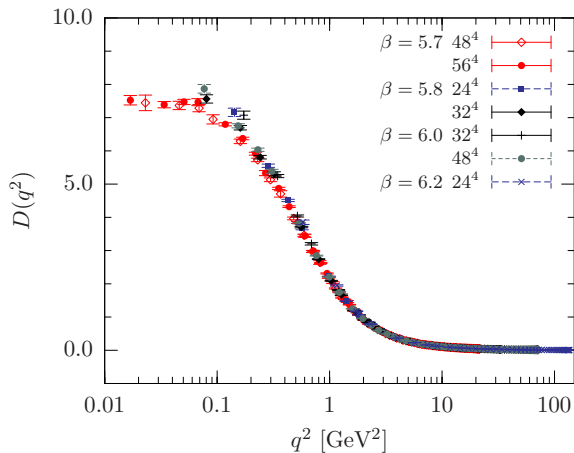


FIG. 3: The gluon propagator  $D(q^2)$  vs.  $q^2$  for quenched QCD, measured on  $f_c$  gauge copies.

possible  $\beta$  value we tried to probe the infrared limit, but with the reservation that the results can be affected by lattice discretization artifacts. To match our lattice results to physical units we used the parametrization of the lattice spacing  $a$  depending on  $\beta$  as determined in [42]. For the full QCD case we have used Hybrid Monte Carlo generated QCDSF gauge field configurations produced with  $N_f = 2$  dynamical flavors of clover-improved Wilson fermions. The relevant parameter sets [35, 36] are listed in Table I. As lattice size we used always  $24^3 \times 48$ . Note that the asymmetry demands some caution in the very infrared.

The gluon dressing function  $Z(q^2)$  and the ghost one  $J(q^2)$  are shown versus  $q^2$  in physical units in Fig. 1 and Fig. 2, respectively, always for the  $f_c$  copies only. The data represent the current status of our quenched and full QCD calculations. In particular, for the quenched case we have included very new results for the gluon propagator obtained at  $\beta = 5.7$  using the lattice sizes  $48^4$  and  $56^4$ . All dressing functions have been

TABLE I: The parameter sets  $\beta$ ,  $\kappa$  etc. for the configurations used in our full QCD investigation (courtesy of the QCDSF collaboration).

$\beta$	$\kappa$	$\kappa_c$	$ma$	$a[\text{GeV}^{-1}]$	# conf
5.29	0.13550	0.136410 (09)	0.0246	2.197	60
5.29	0.13590	0.136410 (09)	0.0138	2.324	55
5.25	0.13575	0.136250 (07)	0.0135	2.183	60

renormalized separately for each  $\beta$  such that they equal unity at  $q = 4 \text{ GeV}$ .

At a first glance our data for the gluon dressing function seem to be qualitatively in agreement with an infrared suppression, whereas the ghost dressing function looks compatible with an infrared singularity. The unquenching effect is clearly visible for the gluon propagator, whereas the ghost propagator is almost unaffected by including the fermionic feed-back in the functional measure of the gluons. This does not come unexpected since the ghost fields do not directly couple to the fermion fields. The non-perturbative peak of the gluon dressing function at  $q \simeq 1 \text{ GeV}$  becomes softer as the quark mass is decreasing. It should be recalled that the gluon peak is wholly removed when center vortices are removed from the gluon field [43]. The corresponding effect of dynamical quarks has been observed also in other lattice computations of the gluon propagator using dynamical AsqTad improved staggered quarks [31] and is expected from studies of the unquenched ghost and gluon propagators within the DSE approach [44, 45, 46]. We refer also to lattice studies with dynamical Kogut-Susskind and Wilson fermions reported in [32, 33] and to the contribution given by S. Furui during this meeting [38].

For the gluon as well as for the ghost dressing functions in the quenched case, with somewhat improved data in comparison to [28], we have tried fits of a power-like infrared behavior (see [1]). For the ghost dressing function the result is indicated in the l.h.s. of Fig. 2. The resulting exponent turned out to be quite stable against variations of the upper end of the fit interval  $q_i^2$ . We have found  $\lambda = 0.20(1)$ , *i.e.* much smaller than expected from the DSE approach. A similar observation was made for the gluon exponent. However, in order to check whether the gluon propagator really vanishes in the infrared — in accordance with the Gribov-Zwanziger horizon condition — we show the gluon propagator itself in Fig. 3. With our new quenched  $SU(3)$  data obtained at  $\beta = 5.7$  on a  $56^4$  lattice we now find a first indication for having reached a maximum, opening the opportunity for a decreasing gluon propagator for even lower momenta. Our results do not seem to expose dramatic finite-size effects, but obviously one needs much larger lattices in order to reach momenta well below 100 MeV. Therefore, it is premature to attempt fits of the infrared exponents with the hope to reproduce the DSE results (see Eq. (1)). This certainly also holds for the ghost propagator, *i.e.* the  $\lambda$  value quoted above cannot be taken seriously.

#### IV. GHOST-GLUON-VERTEX FUNCTION AND THE RUNNING COUPLING

In Fig. 4 we show the running coupling according to Eq. (2). Surprisingly, the coupling is seen to decrease below  $q^2 \simeq 0.3 \text{ GeV}^2$  rather than to approach the predicted non-trivial infrared fix-point monotonously from below. The same happens as well for the quenched as for the unquenched case, irrespective of the clearly visible unquenching effects. Whether strong finite-size effects in the ghost propagator may change the present tendency remains to be seen in future. From our checks of finite-size effects (see below) we cannot derive arguments that this will be the case. It is worth mentioning here that lattice computations of the running coupling from other vertex functions have provided quite similar results (see [47, 48] for the three-gluon vertex and [49] for the quark-gluon vertex).

The definition of the running coupling relies on the assumption of a constant ghost-gluon-vertex renormalization function  $Z_1(q^2)$ . A recent lattice investigation of this function defined at vanishing gluon momentum for the  $SU(2)$  case [18] supports that  $Z_1(q^2) \approx 1$  at least for momenta larger than 1 GeV. We have performed an analogous study for  $Z_1(q^2)$  in the case of  $SU(3)$  gluodynamics and for full QCD. Our results are presented in Fig. 5. There is a slight variation visible in the interval  $0.3 \text{ GeV}^2 \leq q^2 \leq 5 \text{ GeV}^2$ . However, this weak deviation from being constant would not have a dramatic influence on the running coupling.

The left-most two data points falling below unity on the r.h.s. of Fig. 5 correspond to the lowest on-axis momentum on the (asymmetric)  $24^3 \times 48$  lattice. We believe that this deviation is due to the asymmetry of the lattice, because we have seen a similar effect (not shown) in our quenched data, too. Simulations on larger (symmetric) lattices will enable us to sharpen our conclusions within the near future.

#### V. SYSTEMATIC LATTICE AND GRIBOV COPY EFFECTS

It is a common problem of all lattice computations that one has to check the sensitivity of the results with respect to finite-size effects, to the boundary conditions adopted, to an eventual lattice asymmetry, and to the given lattice discretization. We discuss three of these checks in the following. Note that we have employed some cuts on the list of momenta used in order to minimize effects of the lattice discretization from the beginning (see [22],[1]).

In Fig. 6 we demonstrate how the finite lattice size can influence the propagator results. For several fixed  $\beta$  values, *i.e.* for fixed lattice spacings we check the dependence on the varying volume. For smallest lattices (at smallest lattice spacings for  $\beta = 6.2$ ) we find very strong finite-size effects in both cases as one has expected. But our results show that at larger volumes (at lower  $\beta$  values) the lattice size dependence becomes less dramatic.

As a part of the project we also performed simulations at  $\beta = 6.0$  using various asymmetric lattices. In Fig. 7 we show

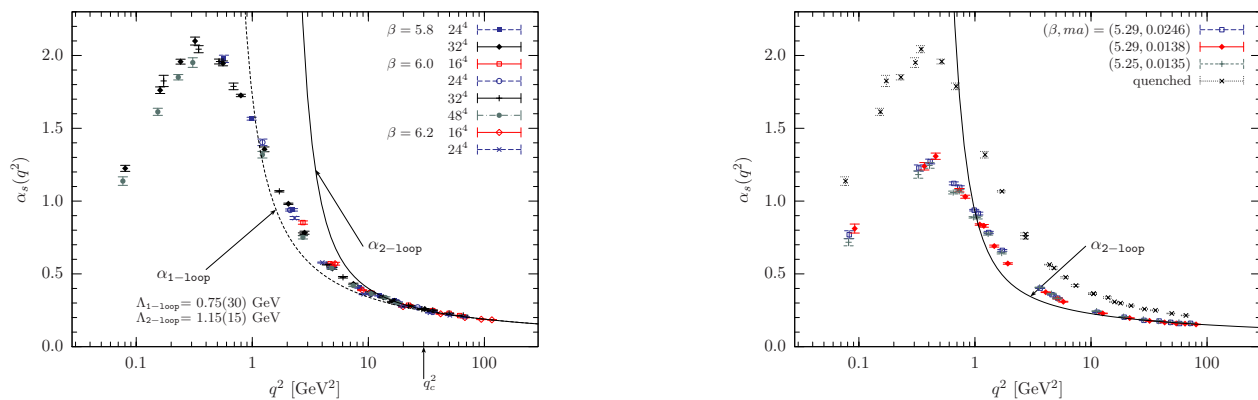


FIG. 4: The momentum dependence of the running coupling  $\alpha_s(q^2)$  for quenched QCD (l.h.s.) and full QCD (r.h.s.), measured on  $fc$  gauge copies. For comparison, on the right hand side selected quenched QCD data for  $\beta = 6.0, 32^4$  are shown. 1- and 2-loop fits to  $\alpha_s(q^2)$  are drawn with dashed and solid lines, respectively.

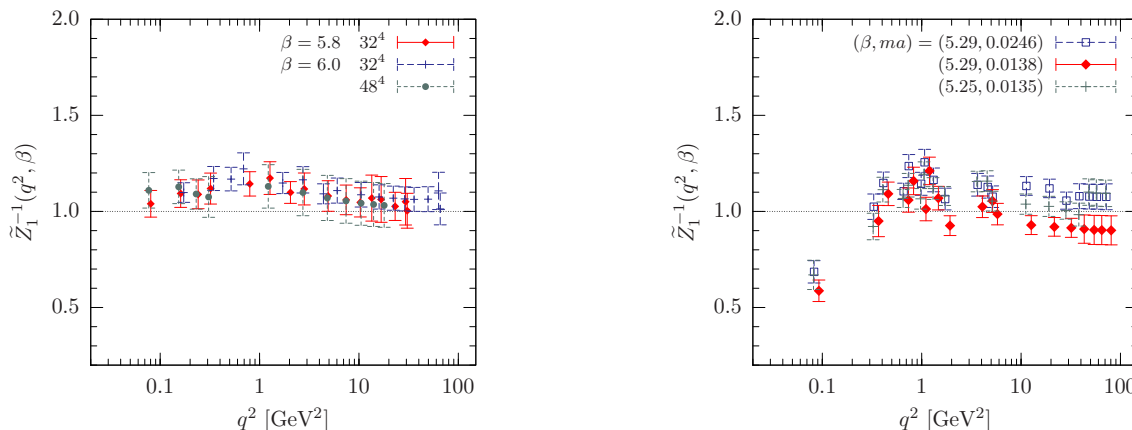


FIG. 5: The inverse ghost-gluon-vertex renormalization function  $Z_1^{-1}(q^2)$ , measured on  $fc$  gauge copies for quenched QCD (l.h.s.) and full QCD (r.h.s.).

gluon (l.h.s.) and ghost (r.h.s.) dressing function data obtained for lattice sizes  $16^3 \times 128$  and  $24^3 \times 128$  in comparison with the symmetric lattice  $48^4$ . We see large systematic effects at low momenta due to the asymmetry, in particular, for the lowest on-axis momenta along the elongated time direction. For a more detailed study of this effect see [1]. Similar observations have been made from 3d  $SU(2)$  investigations in [50]. At this workshop P. Silva has reported on the possibility to use the asymmetry effect for an extrapolation towards the large volume limit [51, 52]. It remains to be seen, whether such an extrapolation really gives stable results.

Next, in Fig. 8 we present a check of the dependence on the lattice discretization for the ghost and the gluon dressing functions in quenched QCD. Whereas the lattice volumes are approximately the same, the lattice spacing changes from  $a \simeq 0.136$  fm ( $\beta = 5.8$ ) to  $a \simeq 0.093$  fm ( $\beta = 6.0$ ). The comparison shows that lattice discretization effects are almost negligible (for the ghost) or quite moderate (for the gluon) in the given momentum interval for the set of (preselected) lattice momenta.

Finally, in Fig. 9 we illustrate the effect of the Gribov copies for periodic gauge transformations. We have plotted some  $fc$  – to –  $bc$  ratios of the ghost and gluon dressing functions. For the gluon propagator there is no influence revealing itself on top of the statistical noise. On the contrary, for the ghost propagator the Gribov problem can cause  $O(5\%)$  deviations in the low momentum region ( $q < 1$  GeV). For better gauge copies the ghost dressing function becomes less singular in the infrared. A closer inspection of the data for the ghost propagator indicates that the influence of Gribov copies becomes weaker for *increasing* physical volume. This probably corroborates a recent claim by Zwanziger telling that in the infinite volume limit averaging over gauge copies in the Gribov region should lead to the same result as averaging over copies restricted to the fundamental modular region [53]. In [54] we have investigated for  $SU(2)$  gluodynamics the effect of admitting a non-periodic extension (modulo  $Z(2)$  flips) of the usually periodic gauge transformations. Also in this case we found that the effect on the Greens functions of the bias towards a particular gauge copy fades away with increasing lattice

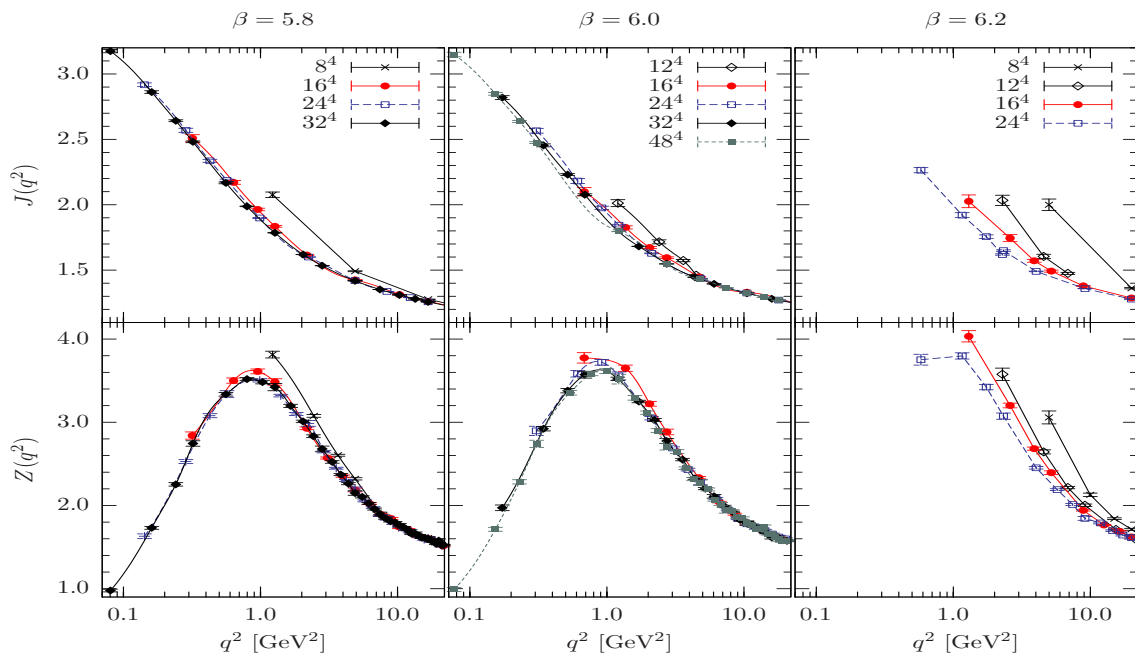


FIG. 6: Demonstration of finite-size effects of the dressing functions for the ghost (upper row) and for the gluon (lower row) in quenched QCD.

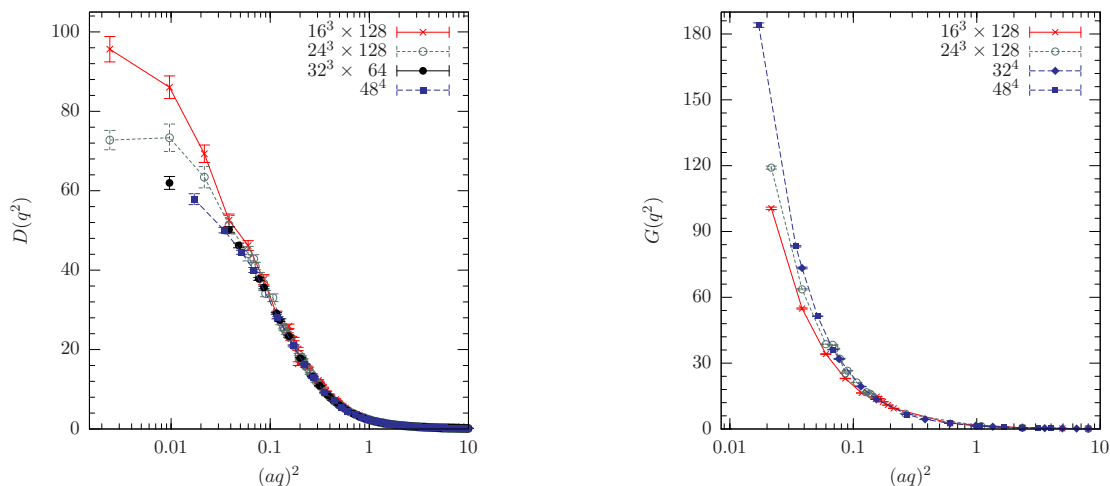


FIG. 7: Lattice asymmetry effects for the gluon (l.h.s.) and ghost (r.h.s.) propagators, respectively, in quenched QCD ( $\beta = 6.0$ , only  $fc$  gauge copies). Note that we have dropped data points at even lower momentum (on-axis in the elongated time direction). Our intention here is to concentrate on the momentum range where we can compare with data obtained on symmetric lattices.

tice volume. Anyway, we see that Gribov copy effects have to be studied properly in the infrared limit before one can come to final conclusions.

## VI. SUMMARY

We have studied the low momentum region of QCD in the Landau gauge using Monte Carlo simulations with the Wilson plaquette action. For the quenched case we could afford to

simulate on lattice sizes ranging from  $8^4$  up to  $56^4$  using bare couplings constants  $\beta$  in the interval  $[5.7, \dots, 6.2]$ . In this way we have presently reached momenta down to  $q \simeq 100$  MeV. In order to assess the effect of virtual quarks we have carried out an analogous investigation for full QCD with two flavors of clover-improved dynamical Wilson fermions for three different quark masses. For the time being we have evaluated only lattices of size  $24^3 \times 48$ . Our data presented here refer to an arbitrary (the “first”) gauge copy as obtained from over-relaxation or Fourier accelerated gauge fixing.

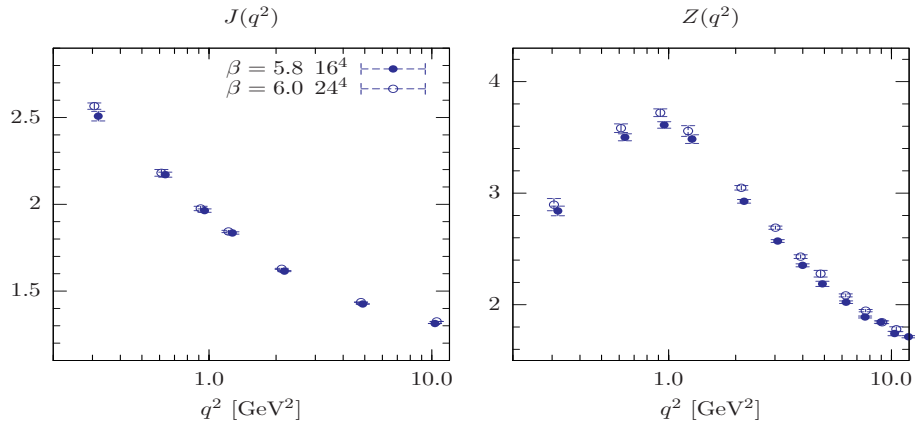


FIG. 8: Lattice discretization effects of the ghost (l.h.s.) and gluon (r.h.s.) dressing functions, respectively, in the quenched case. Both dressing functions are shown for two cases ( $\beta = 5.8, 16^4$  and  $\beta = 6.0, 24^4$ ) corresponding to approximately the same lattice volume  $\simeq (2.2 \text{ fm})^4$ .

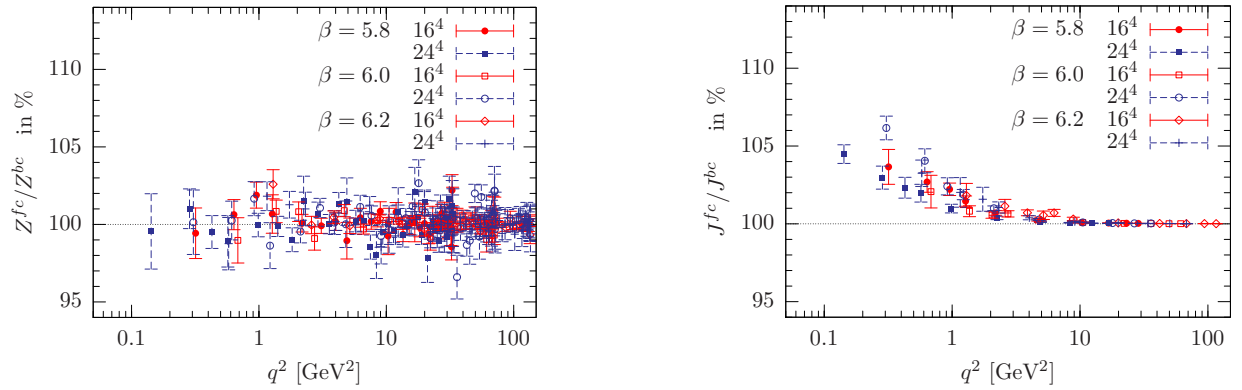


FIG. 9: The ratios  $Z^{fc}/Z^{bc}$  for the gluon dressing functions (l.h.s.) and  $J^{fc}/J^{bc}$  for the ghost dressing functions (r.h.s.) determined on first (fc) and best (bc) gauge copies, respectively, as function of the momentum  $q^2$ .

Towards the infrared momentum region, the gluon dressing functions in quenched as well as in full QCD were shown to decrease, while the ghost dressing functions turned out to rise. However, the interrelated power laws predicted by the infinite-volume DSE approach could not (yet) be confirmed on the basis of our data. Our new data in the quenched case obtained for lattice sizes  $48^4$  and  $56^4$  at  $\beta = 5.7$  demonstrate that the gluon propagator flattens for  $q^2 < 0.1 \text{ GeV}^2$  leaving open the possibility for its decrease at even lower momenta.

From the present data, the running coupling  $\alpha_s(q^2)$  in the momentum subtraction scheme (based on the ghost-gluon vertex) does not seem to approach the expected finite infrared fixed point monotonously. It was rather seen to decrease for lower momenta after passing a turnover at  $q^2 \simeq 0.3 \text{ GeV}^2$  for quenched ( $N_f = 0$ ) as well as for full QCD ( $N_f = 2$ ).

Unquenching effects have been clearly identified for the gluon propagator, whereas the ghost propagator was almost unchanged. This is in one-to-one correspondence with what has been found in the Dyson-Schwinger equation approach. However, the puzzle of the existence of a non-trivial infrared fixed point in the infinite volume limit remains unsolved.

We have studied lattice effects as far as the dependence on the finite lattice size, on the lattice spacing and on the lattice asymmetry are concerned. Within the parameter range under study the first two problems seem to be under control, whereas infinite volume extrapolations based on the strong dependence on the lattice asymmetry might be worth to be further studied.

Concerning the effect of Gribov copies we have seen a quite strong influence in the infrared region on the ghost propagator which becomes less singular when better gauge copies are taken. We have found some indications that the Gribov effect weakens as the volume increases.

## ACKNOWLEDGMENTS

All simulations were done on the IBM pSeries 690 at HLRN and on the MVS-15000BM at the Joint Supercomputer Center (JSCC) in Moscow. This work was supported by the DFG under the contract FOR 465 (Forschergruppe Lattice Hadron Phenomenology), by the DFG-funded graduate school GK 271 and with joint grants DFG 436 RUS 113/866/0 and RFBR 06-02-04014. We thank the QCDSF collabora-

tion for providing us their unquenched configurations which we could access within the framework of the I3 Hadron-Physics Initiative (EU contract RII3-CT-2004-506078). We are grateful to Hinnerk Stüben for contributing parts of the program code. We also acknowledge useful discussions with

R. Alkofer, A. Cucchieri, G. Burgio, C. Fischer, A. Maas, T. Mendes, V. K. Mitrjushkin, O. Oliviera, P. Silva, and D. Zwanziger. M. M.-P. expresses his gratitude to the organizers of ‘Infrared QCD in Rio’ for the kind hospitality and the fruitful workshop atmosphere.

- 
- [1] A. Sternbeck (2006), Ph.D. thesis, hep-lat/0609016.
- [2] L. von Smekal, R. Alkofer, and A. Hauck, Phys. Rev. Lett. **79**, 3591 (1997), hep-ph/9705242.
- [3] L. von Smekal, A. Hauck, and R. Alkofer, Ann. Phys. **267**, 1 (1998), hep-ph/9707327.
- [4] R. Alkofer and L. von Smekal, Phys. Rept. **353**, 281 (2001), hep-ph/0007355.
- [5] J. C. R. Bloch, Phys. Rev. **D64**, 116011 (2001), hep-ph/0106031.
- [6] C. S. Fischer, R. Alkofer, and H. Reinhardt, Phys. Rev. **D65**, 094008 (2002), hep-ph/0202195.
- [7] C. S. Fischer and R. Alkofer, Phys. Lett. **B536**, 177 (2002), hep-ph/0202202.
- [8] C. S. Fischer, Ph.D. thesis, Tübingen University (2003), hep-ph/0304233.
- [9] C. S. Fischer and J. M. Pawłowski (2006), hep-th/0609009.
- [10] J. M. Pawłowski, D. F. Litim, S. Nedelko, and L. von Smekal, Phys. Rev. Lett. **93**, 152002 (2004), hep-th/0312324.
- [11] C. Lerche and L. von Smekal, Phys. Rev. **D65**, 125006 (2002), hep-ph/0202194.
- [12] D. Zwanziger, Phys. Rev. **D65**, 094039 (2002), hep-th/0109224.
- [13] D. Zwanziger, Nucl. Phys. **B412**, 657 (1994).
- [14] V. N. Gribov, Nucl. Phys. **B139**, 1 (1978).
- [15] T. Kugo and I. Ojima, Prog. Theor. Phys. Suppl. **66**, 1 (1979).
- [16] J. C. Taylor, Nucl. Phys. **B33**, 436 (1971).
- [17] W. J. Marciano and H. Pagels, Phys. Rept. **36**, 137 (1978).
- [18] A. Cucchieri, T. Mendes, and A. Mihara, JHEP **12**, 012 (2004), hep-lat/0408034.
- [19] D. V. Shirkov, Theor. Math. Phys. **132**, 1309 (2002), hep-ph/0208082.
- [20] J. C. R. Bloch, A. Cucchieri, K. Langfeld, and T. Mendes, Nucl. Phys. **B687**, 76 (2004), hep-lat/0312036.
- [21] D. B. Leinweber, J. I. Skullerud, A. G. Williams, and C. Parrinello (UKQCD), Phys. Rev. **D58**, 031501 (1998), hep-lat/9803015.
- [22] D. B. Leinweber, J. I. Skullerud, A. G. Williams, and C. Parrinello (UKQCD), Phys. Rev. **D60**, 094507 (1999), hep-lat/9811027.
- [23] F. D. R. Bonnet, P. O. Bowman, D. B. Leinweber, and A. G. Williams, Phys. Rev. **D62**, 051501 (2000), hep-lat/0002020.
- [24] F. D. R. Bonnet, P. O. Bowman, D. B. Leinweber, A. G. Williams, and J. M. Zanotti, Phys. Rev. **D64**, 034501 (2001), hep-lat/0101013.
- [25] S. Furui and H. Nakajima, Phys. Rev. **D69**, 074505 (2004), hep-lat/0305010.
- [26] S. Furui and H. Nakajima, Phys. Rev. **D70**, 094504 (2004), hep-lat/0403021.
- [27] P. Boucaud et al. (2005), hep-ph/0507104.
- [28] A. Sternbeck, E.-M. Ilgenfritz, M. Müller-Preussker, and A. Schiller, Phys. Rev. **D72**, 014507 (2005), hep-lat/0506007.
- [29] A. Sternbeck, E.-M. Ilgenfritz, and M. Müller-Preussker, Phys. Rev. **D73**, 014502 (2006), hep-lat/0510109.
- [30] A. Sternbeck, E.-M. Ilgenfritz, M. Müller-Preussker, and A. Schiller, PoS **LAT2005**, 333 (2005), hep-lat/0509090.
- [31] P. O. Bowman, U. M. Heller, D. B. Leinweber, M. B. Parappilly, and A. G. Williams, Phys. Rev. **D70**, 034509 (2004), hep-lat/0402032.
- [32] S. Furui and H. Nakajima (2005), hep-lat/0503029.
- [33] S. Furui and H. Nakajima, PoS **LAT2005**, 291 (2005), hep-lat/0509035.
- [34] E.-M. Ilgenfritz, M. Müller-Preussker, A. Sternbeck, and A. Schiller (2006), hep-lat/0601027.
- [35] M. Göckeler et al. (QCDSF), Phys. Lett. **B639**, 307 (2006), hep-ph/0409312.
- [36] M. Göckeler et al., Phys. Rev. **D73**, 014513 (2006), hep-ph/0502212.
- [37] A. Cucchieri and T. Mendes (2006), hep-ph/0605224.
- [38] S. Furui and H. Nakajima (2006), hep-lat/0609024.
- [39] A. Sternbeck, E. M. Ilgenfritz, M. Müller-Preussker, A. Schiller, and I. L. Bogolubsky, PoS **LAT2006**, 076 (2006), hep-lat/0610053.
- [40] H. Suman and K. Schilling, Phys. Lett. **B373**, 314 (1996), hep-lat/9512003.
- [41] A. Cucchieri, Nucl. Phys. **B508**, 353 (1997), hep-lat/9705005.
- [42] S. Necco and R. Sommer, Nucl. Phys. **B622**, 328 (2002), hep-lat/0108008.
- [43] K. Langfeld, H. Reinhardt, and J. Gattnar, Nucl. Phys. **B621**, 131 (2002), hep-ph/0107141.
- [44] C. S. Fischer, R. Alkofer, W. Cassing, F. Llanes-Estrada, and P. Watson, Nucl. Phys. Proc. Suppl. **153**, 90 (2006), hep-ph/0511147.
- [45] C. S. Fischer, P. Watson, and W. Cassing, Phys. Rev. **D72**, 094025 (2005), hep-ph/0509213.
- [46] C. S. Fischer and R. Alkofer, Phys. Rev. **D67**, 094020 (2003), hep-ph/0301094.
- [47] P. Boucaud, J. P. Leroy, J. Micheli, O. Pene, and C. Roiesnel, JHEP **10**, 017 (1998), hep-ph/9810322.
- [48] P. Boucaud et al., JHEP **04**, 005 (2003), hep-ph/0212192.
- [49] J. Skullerud and A. Kizilersu, JHEP **09**, 013 (2002), hep-ph/0205318.
- [50] A. Cucchieri and T. Mendes, Phys. Rev. **D73**, 071502 (2006), hep-lat/0602012.
- [51] P. J. Silva and O. Oliveira, Phys. Rev. **D74**, 034513 (2006), hep-lat/0511043.
- [52] O. Oliveira and P. J. Silva (2006), hep-lat/0609027.
- [53] D. Zwanziger, Phys. Rev. **D69**, 016002 (2004), hep-ph/0303028.
- [54] I. L. Bogolubsky, G. Burgio, M. Müller-Preussker, and V. K. Mitrjushkin, Phys. Rev. **D74**, 034503 (2006), hep-lat/0511056.